Hydrogenolysis of epoxy resins by a reusable CeO_2-supported Ni−Pd bimetallic catalyst toward recycling of epoxy thermosets

Yanze Huang[1], Yukari Yamazaki[1], Katsutoshi Nomoto[2], Hiroki Miura[2], Tetsuya Shishido[2], Xiongjie Jin[1]*, Kyoko Nozaki[1]*

[1]Department of Chemistry and Biotechnology, Graduate School of Engineering, The University of Tokyo, 7-3-1 Hongo, Bunkyo-ku, Tokyo 113-8656, Japan

[2]Department of Applied Chemistry for environment, Graduate School of Urban Environmental Sciences, Tokyo Metropolitan University, 1-1 Minami-Osawa, Hachioji, Tokyo 192-0397, Japan

E-mail: t-jin@g.ecc.u-tokyo.ac.jp
nozaki@chembio.t.u-tokyo.ac.jp

Abstract

Recycling of epoxy composites, one of the most widely utilized thermoset plastics, is of importance for achieving circular economy as demand for the lightweight materials in the field of sustainable technologies is soaring. Although catalytic hydrogenolysis of epoxy resins provides a promising approach to recover valuable fillers and phenolic compounds from the composites, there is a lack of a reusable heterogeneous catalyst for this purpose. Here, we report a robust Ni−Pd bimetallic nanoparticles supported on CeO_2 (Ni−Pd/CeO_2) for the hydrogenolysis of epoxy resins under mild conditions (180 °C, 1 atm of H_2). Mechanistic studies revealed that Pd-induced reduction of Ni^{2+} to Ni^0 is the key for the high efficiency of the bimetallic catalyst. Benefiting from its heterogeneous nature, Ni−Pd/CeO_2 can be easily recycled and reused for several times. The catalyst is also applicable to decomposition of carbon fiber-reinforced epoxy resins to recover carbon fibers and bisphenol A, indicating the potential application of our catalyst system toward recycling of epoxy composites.

Introduction

The growing global concerns on plastic waste contamination have urged our society to develop effective ways to recycle end-of life plastics.[1] Epoxy resins, which share the majority of thermoset market, are widely applied in various areas such as construction, electronics, aircrafts, automobiles, and wind turbine blades typically in the form of fiber-reinforced epoxy composites (Figure 1a).[2] Different from thermoplastics such as polyethylene terephthalate, thermosetting epoxy resin composites are not suitable for mechanical recycling due to deterioration of material properties, and thus most of the composites are landfilled which not only wastes resources but also causes serious environmental problems.[3] As the demand for epoxy resin composites are soaring with the increasing demand for lightweight materials in the field of sustainable technologies such as electric vehicles and wind power plant, the development of efficient approaches to recycle epoxy composites is getting more and more attention for achieving circular economy and carbon neutralization.[2,3]

To date, a wide range of methods have been developed for decomposition of epoxy composites (Figure 1a).[3] For example, pyrolysis under energy-intensive high temperature conditions is an approach to recover fillers from the composites, which often causes damage to the fillers due to the harsh conditions.[4] Other methods, such as oxidative decomposition[5] using oxidants (e.g., H_2O_2), or solvolysis[6] in concentrated acids (e.g., nitric acid) or bases (e.g., NaOH) has also been developed to deconstruct epoxy resin metrics. However, they have shortcomings of using the undesirable oxidants or a large excess amount of acid or bases which would increase the environmental burden. In addition, all the above methods mainly focus on the recovery of fillers in the composites, and epoxy resin building blocks such as bisphenol A (BPA) are difficult to recover. In this context,

chemical recycling of epoxy resins is of importance to recover valuable fillers together with phenolic compounds from the epoxy composites, but highly challenging due to their inert nature. Recently, it has been revealed that BPA can be recovered from epoxy resins by using a super-stoichiometric amount of potassium *t*-butoxide (4 equiv. with respect to BPA units)[7] or NaOH (6 equiv. with respect to BPA units).[8] However, tedious work-up procedures using a large quantity of acids are necessary to obtain BPA because the primary products are potassium or sodium phenolate.

Quite recently, catalytic reductive decomposition of epoxy resins to recover BPA has received much attention (Figure 1b).[9,10] For example, Ahrens and Skrystrup have reported a homogeneous Ru-based catalyst for decomposition of epoxy resin composites to recover fibers and BPA using 2-propanol as the hydrogen source.[9] Concurrently, our group has developed a homogeneous Ni-based catalyst for hydrogenolysis of epoxy resins to recover BPA using H_2 as the reductant.[10] In spite of the efficiency of these catalyst systems for recovering BPA and fibers from epoxy composites, they suffer from difficulties in catalyst recovery and reuse due to the homogeneous nature of the catalysts, which is problematic especially when noble metal catalysts are employed. Therefore, the development of a robust and reusable heterogeneous catalyst for hydrogenolysis of epoxy resins to recycle epoxy resin composites using readily available H_2 is highly desirable. However, as far as we know,[3−10] there is a lack of a heterogeneous catalyst for decomposition of epoxy composites to recover phenolic compounds and fillers.

Here, for the first time, we successfully developed a reusable Ni−Pd bimetallic nanoparticles supported on CeO_2 (Ni−Pd/CeO_2) for the hydrogenolysis of epoxy resins (Figure 1c). Considering most of epoxy resins utilized nowadays are prepared by curing the BPA-based epoxide prepolymer with amines or acid anhydrides (Figure 1a),[2,11] the key to recover BPA is the selective hydrogenolysis of C(sp^3)─O bonds in the phenolic ethers without reduction of aromatic rings in the resin backbone. Bimetallic catalysts have widely been applied to the hydrogenolysis of C─O bonds for upgrading biomass such as lignin.[12] Because the basic structure of epoxy resins contains *β*-hydroxy ether moieties sharing similar structures with the *β*-O-4 linkage in lignin,[13] we considered to explore bimetallic catalysts for the hydrogenolysis of epoxy resins. As such, we found that a combination of Ni and Pd showed high activity for the hydrogenolysis of epoxy resins cured with amines or acid anhydrides. The Ni−Pd/CeO_2 catalyst can also be applied to the decomposition of carbon fiber-reinforced epoxy resins (CFRP) to recover carbon fibers and BPA, implying its potential application to recycle epoxy thermosets.

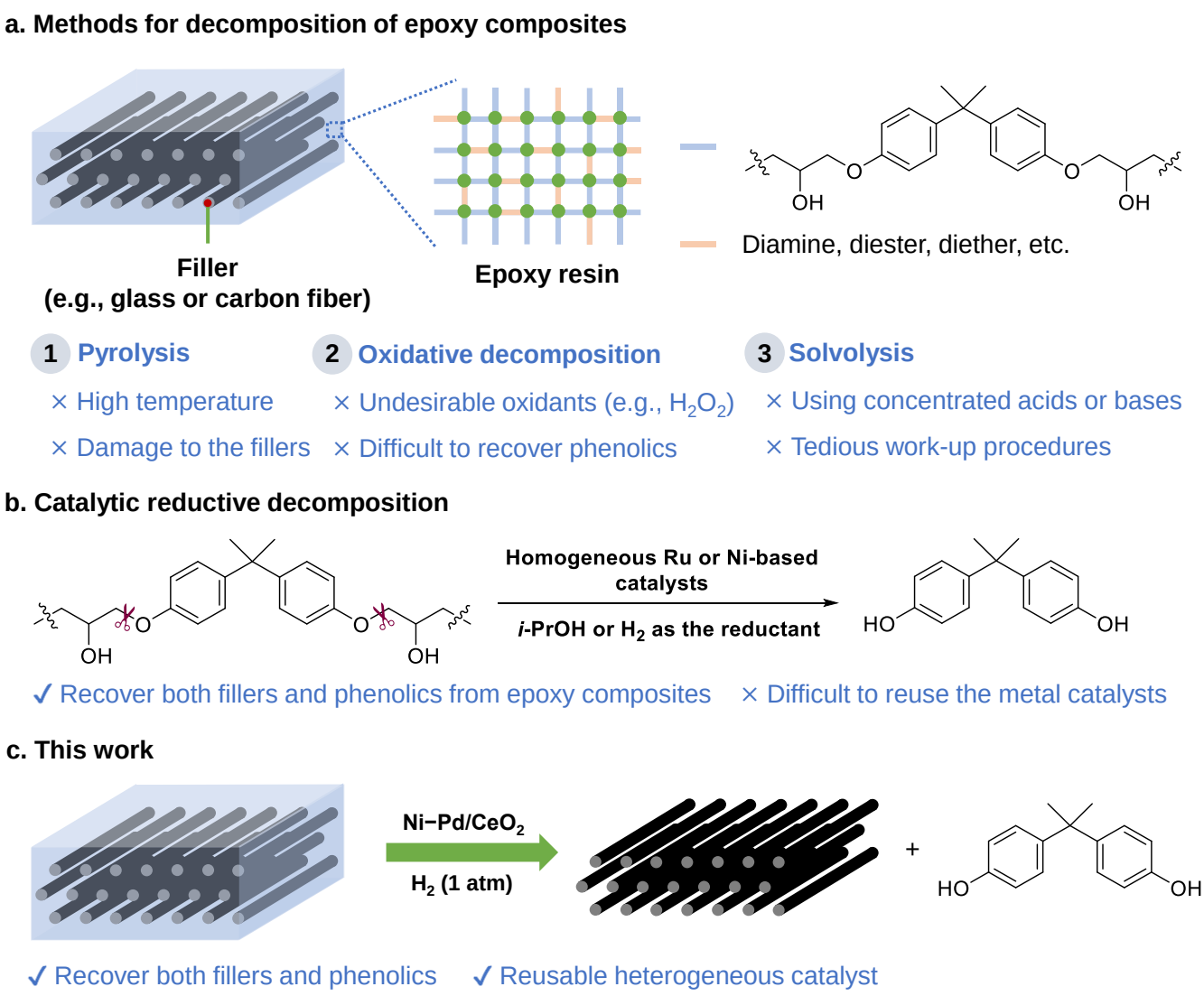

Figure 1. Outline of this work. (a) Structure of typical epoxy resin composites and traditional methods for their decomposition. (b) Catalytic reductive decomposition of epoxy composites using homogeneous Ru or Ni catalysts. (c) This work: decomposition of epoxy composites via hydrogenolysis of epoxy resins using a reusable heterogeneous Ni−Pd/CeO_2 catalyst.

Results and discussion

Catalyst development. Our starting point to develop efficient supported bimetallic catalysts for the hydrogenolysis of the C(sp^3)−O bonds in epoxy resins using H_2 as the hydrogen source is to combine two different metals that are effective for C−O bond cleavage and H_2 activation, respectively. In this context, 3*d* transition metals (Ni, Co, and so on) are known to be active for the C−O bond cleavage,[14] and noble metals such as Pd and Pt are efficient for H_2 activation.[15] In addition, it has been reported that the combination of 3*d* and noble transition metals can efficiently promote the hydrogenolysis of the *β*-O-4 linkage in lignin.[16] Therefore, we initially tried various combinations of 3*d* transition metals and Pd (or Pt) supported on CeO_2 for the selective hydrogenolysis of the C(sp^3)−O bonds in epoxy resin backbone. The supported metal catalysts were prepared either by deposition-precipitation or incipient wetness impregnation method followed by treatment with 1 atm of H_2 at 150 ºC for 0.5 h (the supported metal catalysts are designated as $M_xM'_y$/support, where the ratio of M to M' is *x*/*y*; see Supporting Information for the details of the preparation of the catalysts). Then, the hydrogenolysis of epoxy resin model **1** was carried out in *N*-methylpyrrolidone (NMP) at 180 ºC and under 1 atm of H_2 to evaluate the catalytic activity. Among various CeO_2-supported bimetallic catalysts such as Ni_1Pd_1/CeO_2, Cu_1Pd_1/CeO_2, Co_1Pd_1/CeO_2, Fe_1Pd_1/CeO_2, Mn_1Pd_1/CeO_2, Ni_1Pt_1/CeO_2, and

Fe_1Pt_1/CeO_2, Ni_1Pd_1/CeO_2 showed the highest activity for the hydrogenolysis of **1**, and gave the corresponding hydrogenolysis product, BPA (**2**), in 74% yield along with 4-isopropylphenol (**3**) and phenol (**4**), which are formed by C−C bond cleavage of **2** (Table 1, entries 1−7). Interestingly, the reduction of aromatic rings of phenolic compounds did not occur. The conversion of **1** and the yields of phenols were gradually increased with increasing the amount of the supported Pd species (Table 1, entries 1, 8, and 9). In contrast, there are no substantial change in the conversion or yield when the amount of Ni was increased or decreased (Table 1, entries 1, 10, and 11). The single metallic Ni/CeO_2 or Pd/CeO_2 was not as effective as the Ni−Pd bimetallic catalysts for the hydrogenolysis and gave significantly lower yield of the corresponding hydrogenolysis product(s) (Table 1, entries 12 and 13). Ni−Pd supported on other supports, such as TiO_2, Al_2O_3, or ZrO_2, resulted in much lower conversion and yields than Ni_1Pd_1/CeO_2 (Table 1, entries 14−16). Furthermore, a physical mixture of Ni/CeO_2 and Pd/CeO_2 resulted in a higher activity than Ni/CeO_2 or Pd/CeO_2 alone (Table 1, entry 17 *vs* 12 and 13), but still gave a much lower conversion and yield than Ni_1Pd_1/CeO_2 (Table 1, entry 17 *vs* 1). Therefore, only if Ni together with Pd were directly supported on CeO_2, the activity for the hydrogenolysis was increased dramatically, and the cooperation between Ni and Pd is crucial for the high activity of Ni_1Pd_1/CeO_2. As a control experiment, CeO_2 could not promote the hydrogenolysis of **1** (Table 1, entry 18).

Table 1. Effect of catalysts on the hydrogenolysis of an epoxy resin model

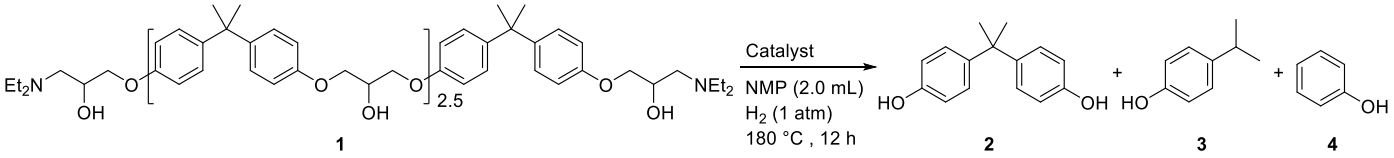

Entry[a]	Catalyst	Conv. of **1** (%)	Yield (%)		
			2	**3**	**4**
1	**Ni_1Pd_1/CeO_2**	**93**	**74**	**19**	**15**
2	Cu_1Pd_1/CeO_2	25	19	1	0
3	Co_1Pd_1/CeO_2	41	25	12	11
4	Fe_1Pd_1/CeO_2	45	21	0	0
5	Mn_1Pd_1/CeO_2	49	38	3	3
6	Ni_1Pt_1/CeO_2	17	14	0	0
7	Fe_1Pt_1/CeO_2	22	6	0	0
8	$Ni_1Pd_{0.1}/CeO_2$	28	12	0	0
9	$Ni_1Pd_{0.5}/CeO_2$	51	36	2	0
10	$Ni_{0.5}Pd_1/CeO_2$	97	70	16	15
11	Ni_2Pd_1/CeO_2	95	77	9	9
12[b]	Ni/CeO_2	11	1	0	0
13[c]	Pd/CeO_2	18	9	2	1
14	Ni_1Pd_1/TiO_2	23	6	0	0
15	Ni_1Pd_1/Al_2O_3	11	4	0	0
16	Ni_1Pd_1/ZrO_2	5	1	0	0
17[b,c]	Ni/CeO_2 + Pd/CeO_2	49	29	4	4
18[d]	CeO_2	3	0	0	0

[a]Reaction conditions: **1** (200 mg, 0.52 mmol BPA unit), $M_xM'_y/CeO_2$ (100 mg; M ≈ 4.2*x* mol%; M' ≈ 4.8*y* mol%, the exact amount of the metal used in the hydrogenolysis is varied slightly depending on the kind of supported metal species), NMP (2.0 mL), 180 °C, H_2 (1 atm, balloon), 12 h. Conversion of **1** and yield of **4** were determined by ^{1}H NMR analysis. Yields of **2** and **3** were determined by GC analysis. [b]Ni/CeO_2 (100 mg, Ni = 4.0 mol%). [c]Pd/CeO_2 (100 mg, Pd = 5.0 mol%). [d]CeO_2 (100 mg).

Characterization of the catalyst. The Ni_1Pd_1/CeO_2 catalyst was characterized by powder X-ray diffraction (XRD), X-ray photoelectron spectroscopy (XPS), X-ray absorption fine structure (XAFS) spectroscopy, and high-angle annular dark-field scanning transmission electron microscopy (HAADF-STEM) analysis. XRD pattern of the catalyst revealed that the structure of CeO_2 was maintained well upon immobilization of Ni and Pd species and the subsequent treatment with H_2 gas (Figure 2a). Furthermore, no apparent diffraction peaks attributable to Pd, Ni, or NiO were observed, indicating Ni and Pd species are highly dispersed on CeO_2 surface (Figure 2a). From the X-ray photoelectron spectroscopy (XPS) analysis of Ni_1Pd_1/CeO_2, the supported Ni−Pd alloy nanoparticles contain Pd^{2+} (336.8 and 342.2 eV), Pd^0 (335.2 and 340.5 eV), Ni^{2+} (855.4 eV), and Ni^0 (852.4 eV) species, and the ratios of Pd^{2+} to Pd^0 and Ni^{2+} to Ni^0 were 17/83 and 79/21, respectively (Figure 2b and 2c). Pd K-edge X-ray absorption near edge structure (XANES) spectrum of

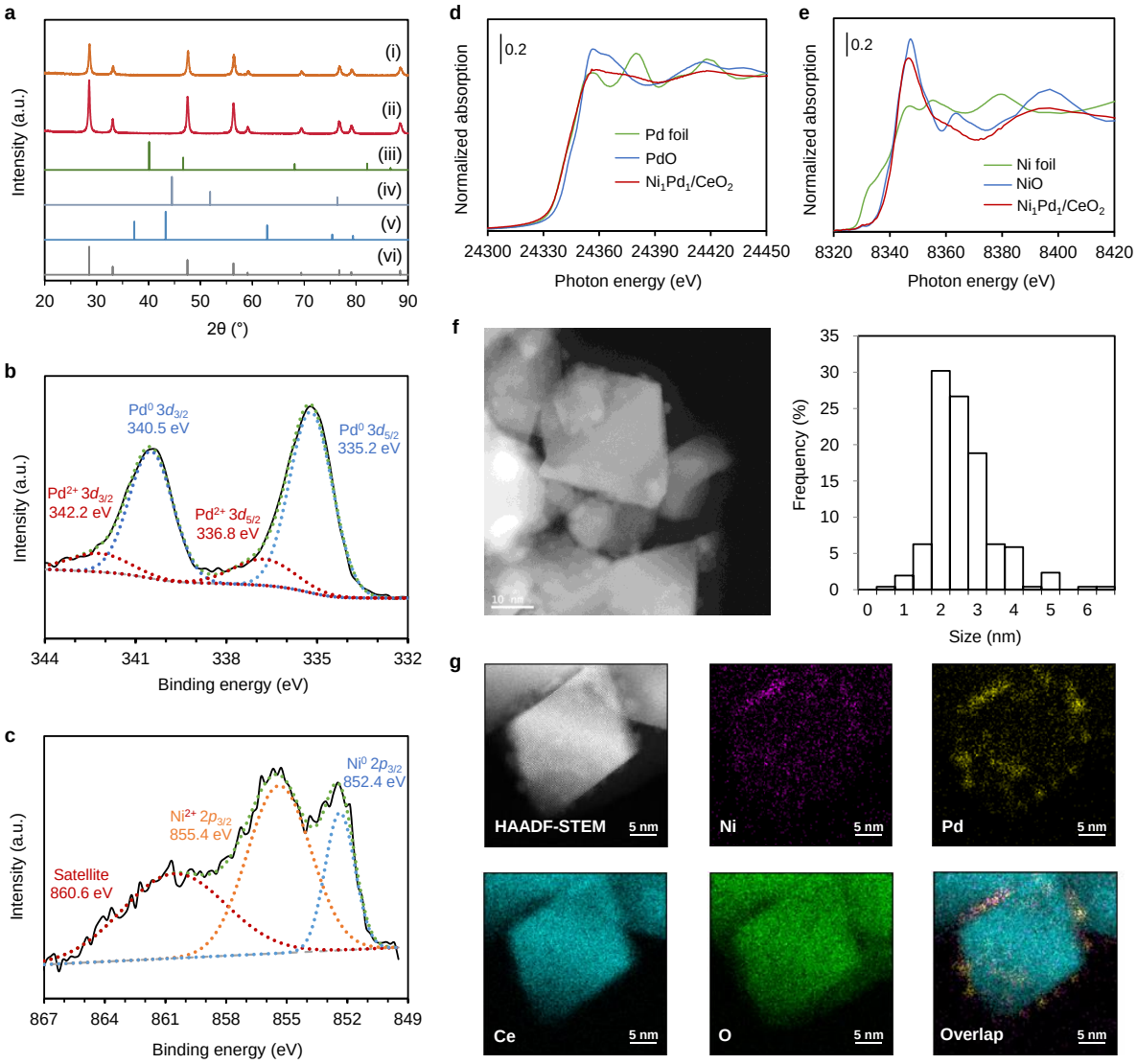

Figure 2. Characterization of the catalysts. (a) XRD patterns of (i) Ni_1Pd_1/CeO_2, (ii) CeO_2, (iii) the powder diffraction file of Pd metal (file No. 8796), (iv) the powder diffraction file of Ni metal (file No. 8783), (v) the powder diffraction file of NiO (file No. 5898), (vi) the powder diffraction file of CeO_2 (file No. 11). (b) XPS spectrum of Ni_1Pd_1/CeO_2 in the region of 332−344 eV (Pd 3*d*). (c) XPS spectrum of Ni_1Pd_1/CeO_2 in the region of 849−867 eV (Ni 2*p*). The black line indicates the original spectrum, the blue, red, and orange broken lines indicate the deconvoluted signals, and the green broken line indicates the sum of the deconvoluted signals. (d) Pd K-edge XANES spectrum. (e) Ni K-edge XANES spectrum. (f) STEM image and particle size distribution of Ni_1Pd_1/CeO_2 (average = 2.6 nm; standard deviation, $\sigma = 0.8$ nm, $n = 256$). (g) HAADF-STEM image and elemental mapping of Ni_1Pd_1/CeO_2 by EDS analysis.

Ni_1Pd_1/CeO_2 showed that the supported Pd is mainly composed of Pd^0 species (Figure 2d). From Ni K-edge XANES spectrum, it is revealed that the catalyst mainly contains Ni^{2+} species (Figure 2e). Therefore, the results obtained from XANES spectra are in good agreement with that from XPS spectra. HAADF-STEM and EDS analysis of the catalyst showed that Ni and Pd species are located on the same position of the catalyst surface, and the average particle size was approximately 2.6 nm (Figure 2f and 2g).

Hydrogenolysis of other epoxy resin model compounds by Ni_1Pd_1/CeO_2. As shown in Scheme 1, Ni_1Pd_1/CeO_2 can efficiently promote the hydrogenolysis of various epoxy model compounds. For model compounds **5**–**7** having hydroxy group adjacent to the ether bonds, the hydrogenolysis proceeded smoothly under 1 atm of H_2, giving the corresponding hydrogenolysis product **9** in high yields (Scheme 1). When the hydrogenolysis of **5** was carried out in the presence of tributylamine, substantial amounts of the C–C bond-cleaved products such as **3** (45%), **4** (13%), and anisole (29%) were obtained (Scheme S1). Therefore, the amine moiety in model **1** resulted in the formation of **3** and **4** for the hydrogenolysis of **1** (Table 1, entry 1).

The hydrogenolysis of models **5**–**7** also proceeded under N_2 with lower yields of **9** produced, indicating the transfer hydrogenolysis proceeds for which the hydroxy groups would serve as the hydrogen source. In addition, the hydrogenolysis of the ether without the hydroxy group did not proceed at all, suggesting that the hydroxy group is indispensable for the hydrogenolysis of the ether bonds (Scheme 1, model **8**). The reason for the necessity of the hydroxy group is discussed in the following section.

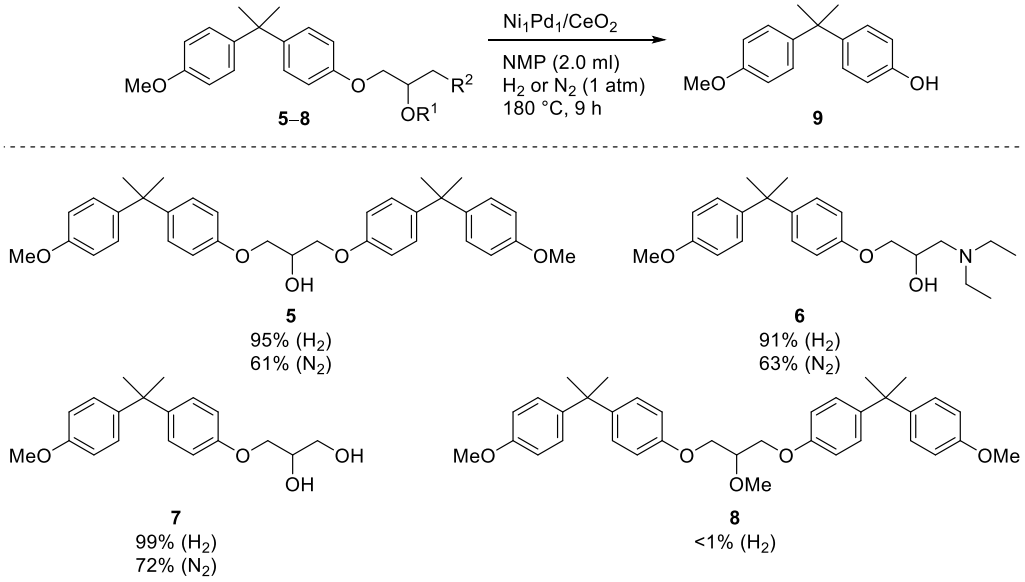

Scheme 1. Hydrogenolysis of various epoxy resin model compounds by Ni_1Pd_1/CeO_2. Reaction conditions: model **5** or **8** (0.25 mmol), Ni_1Pd_1/CeO_2 (100 mg), NMP (2.0 mL), 180 °C, H_2 (1 atm, balloon), 9 h. For model **6** or **7**, 0.50 mmol of the substrate was used. The catalyst was pre-treated with 1 atm of H_2 at 150 °C for 0.5 h. The yields of **9** are shown here for the hydrogenolysis of each model compound under H_2 or N_2. The yields were determined by GC analysis.

Mechanistic studies. The reaction pathway for the present hydrogenolysis was investigated. As mentioned above, the hydrogenolysis of models **5**–**7** proceeded even under N_2 and model **8** did not react at all (Scheme 1). Therefore, as shown in Figure 3a, it is likely that the hydrogenolysis proceeds through dehydrogenation of the alcohol moiety to form the corresponding ketone intermediate followed by hydrogenolysis of the C–O bond adjacent to the carbonyl group. The proposed reaction pathway was further supported by the hydrogenolysis of models **10** and **11** (Figure 3b). When the hydrogenolysis of **10** was carried out at 180 °C

and under 1 atm of H_2 for 6 h, full conversion of **10** gave **9**, 2-tetradecanone (**12**), and 2-tetradecanol (**13**) in 91%, 80%, and 14% yield, respectively (Figure 3b (i), entry 1). Notably, when Ni/CeO_2 was used as the catalyst, the dehydrogenated ketone intermediate **11** was detected (Figure 3b (i), entry 3). In addition, the hydrogenolysis of **11** using Ni_1Pd_1/CeO_2 proceeded smoothly (Figure 3b (ii), entry 1), supporting the reaction proceeds through the ketone intermediate as shown in Figure 3a. Also, the formation of **10** during the hydrogenolysis of **11** suggests that an equilibrium between **10** and **11** exists *via* dehydrogenation and hydrogenation (Figure 3b (ii), entries 1 and 3).

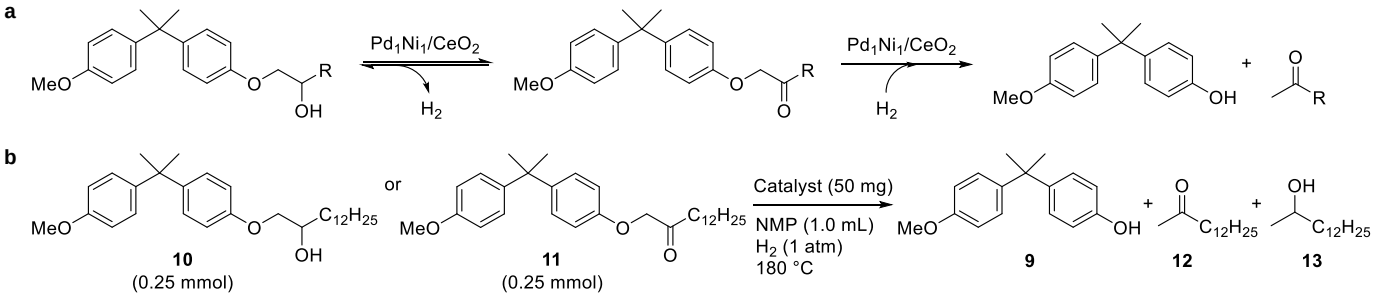

i **Model 10 as the substrate (reaction time = 6 h)**

Entry[a]	Catalyst	Conv. of **10** (%)	Yield (%)			
			9	**12**	**13**	**11**
1	Ni_1Pd_1/CeO_2	>99	91	80	14	n.d.
2	Pd/CeO_2	24	23	21	1	n.d.
3	Ni/CeO_2	17	5	2	n.d.	12

ii **Model 11 as the substrate (reaction time = 4 h)**

Entry[a]	Catalyst	Conv. of **11** (%)	Yield (%)			
			9	**12**	**13**	**10**
1	Ni_1Pd_1/CeO_2	>99	94	86	8	5
2	Pd/CeO_2	94	85	87	n.d.	n.d.
3	Ni/CeO_2	76	8	7	1	68

[a]The catalyst was treated with 1 atm of H_2 at 300 °C for 1 h. Conversion and yield of **10** and **11** were determined by 1H NMR analysis. Yields of **9**, **12**, and **13** were determined by GC analysis. n.d. = not detected.

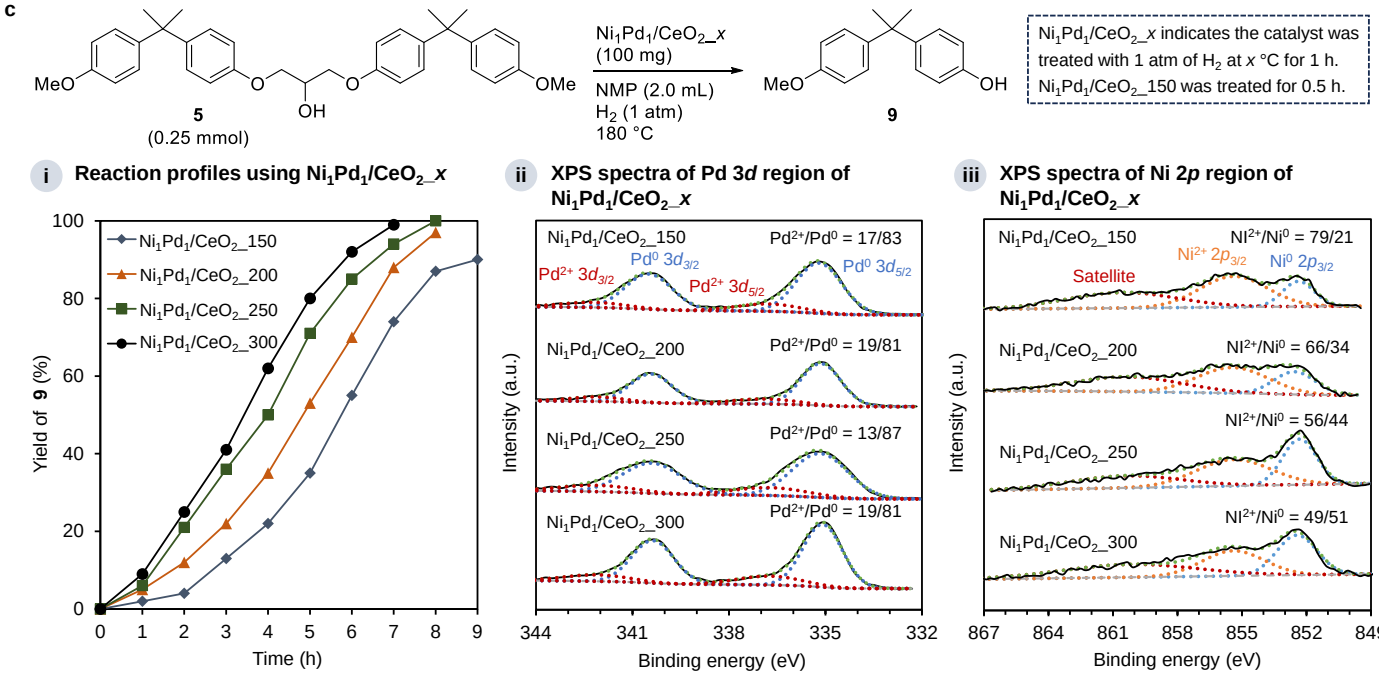

Figure 3. Mechanistic studies. (a) Proposed reaction pathway for the hydrogenolysis. (b) Hydrogenolysis of models **10** and **11** using Ni_1Pd_1/CeO_2, Pd/CeO_2, and Ni/CeO_2. (c) The hydrogenolysis of model **5** using Ni_1Pd_1/CeO_2 treated under different temperatures. (i) reaction profiles; (ii) XPS spectra of the catalysts in Pd 3*d* region; (iii) XPS spectra of the catalysts in Ni 2*p* region. The black line indicates the original spectrum, the blue, red, and orange broken lines indicate the deconvoluted signals, and the green broken line indicates the sum of the deconvoluted signals.

Next, the role of the supported Ni and Pd species for the hydrogenolysis was investigated. For the hydrogenolysis of **11**, Pd/CeO_2 resulted in almost the same conversion and yields as Ni_1Pd_1/CeO_2 (Figure 3b (ii), entry 1 *vs* entry 2), but is much more active than Ni/CeO_2 (Figure 3b (ii), entry 2 *vs* entry 3), indicating the supported Pd species are highly active and mainly responsible for the hydrogenolysis of the C−O bond. On the other hand, Pd/CeO_2 showed much lower activity than Ni_1Pd_1/CeO_2 for the hydrogenolysis of **10** (Figure 3b (i), entry 1 *vs* entry 2), which suggests the Pd species alone have lower efficiency for the dehydrogenation step, and Ni together with Pd substantially promote the dehydrogenation of **10** to **11**.

For the hydrogenolysis of model **5**, an induction period was observed (Figure 3c (i), and Figure S1). To investigate the origin of the induction period, we pretreated Ni_1Pd_1/CeO_2 with 1 atm of H_2 at different temperatures, and the hydrogenolysis of **5** was carried out using these catalysts. The reaction profiles showed that the induction period was decreased with increase of the pre-treatment temperature (Figure 3c (i)). XPS analysis of the catalysts showed that the ratio of Pd^{2+} to Pd^0 was approximately the same when the catalysts were treated at different temperatures. However, the ratio of Ni^{2+} to Ni^0 was decreased from 79/21 to 49/51, indicating a substantially larger amount of Ni^{2+} species was reduced to Ni^0 at higher pre-treatment temperature. Therefore, the supported Ni species rather than Pd species are related to the induction period, and the higher amount of the surface Ni^0 species resulted in the shorter induction period. This result was further supported by the following experiments. When Ni_1Pd_1/CeO_2 treated at 150 °C was recovered after the hydrogenolysis of **5** for 2 h, the ratio of Ni^{2+} to Ni^0 was decreased from 79/21 to 57/43, and the ratio was kept almost unchanged until the end of the reaction (61/30), supporting that Ni^{2+} was reduced to Ni^0 during the induction period (Figure S2).

In our bimetallic catalyst system, Pd induces the reduction of Ni^{2+} to Ni^0. When Ni/CeO_2 was reduced with 1 atm of H_2 at 300 °C for 1 h, the ratio of Ni^{2+} to Ni^0 was 73/27 (Figure S3). On the other hand, the ratio was 49/51 for Ni_1Pd_1/CeO_2 reduced under the same conditions, supporting a larger amount of Ni^{2+} was reduced to Ni^0 in the presence of Pd. As the supported Pd species rather than Ni species play the major role for the hydrogenolysis of the C−O bond in the ketone intermediate **11**, the reduction of Ni^{2+} to Ni^0 is indispensable for promoting the dehydrogenation of the alcohol moiety. Overall, the Pd-induced reduction of Ni^{2+} to Ni^0 enhances the rate of the dehydrogenation step shown in Figure 3a. Consequently, the bimetallic Ni_1Pd_1/CeO_2 is more efficient than the corresponding single metallic catalysts for the hydrogenolysis of the *β*-hydroxy ether moieties in epoxy resins.

Hydrogenolysis of epoxy resins and decomposition of CFRP. The applicability of our catalyst system was demonstrated by the hydrogenolysis of epoxy resins and decomposition of an epoxy composite, CFRP. As shown in Scheme 2, Ni_1Pd_1/CeO_2 was successfully applied to the hydrogenolysis of acid anhydride or amine-cured epoxy resin. For the hydrogenolysis of acid anhydride-cured epoxy resin, a catalytic amount of 1,8-diazabicyclo[5.4.0]undec-7-ene (DBU) was added to promote the decomposition,[17] and BPA was obtained in 52% yield (Scheme 2a). The hydrogenolysis of an amine-cured epoxy resin also proceeded efficiently in the presence of a catalytic amount of K_3PO_4 (Scheme 2b). In this case, BPA (**2**) was not obtained. Instead, C−C bond cleavage occurred to give 4-isopropylphenol and phenol in 99% and 81% yield, respectively. As described above, the aliphatic tertiary amine moiety in the epoxy resin is responsible for the C−C bond cleavage. More importantly, the present catalyst system can be applied to the decomposition of CFRP, by which BPA and carbon fiber was successfully recovered from the CFRP.

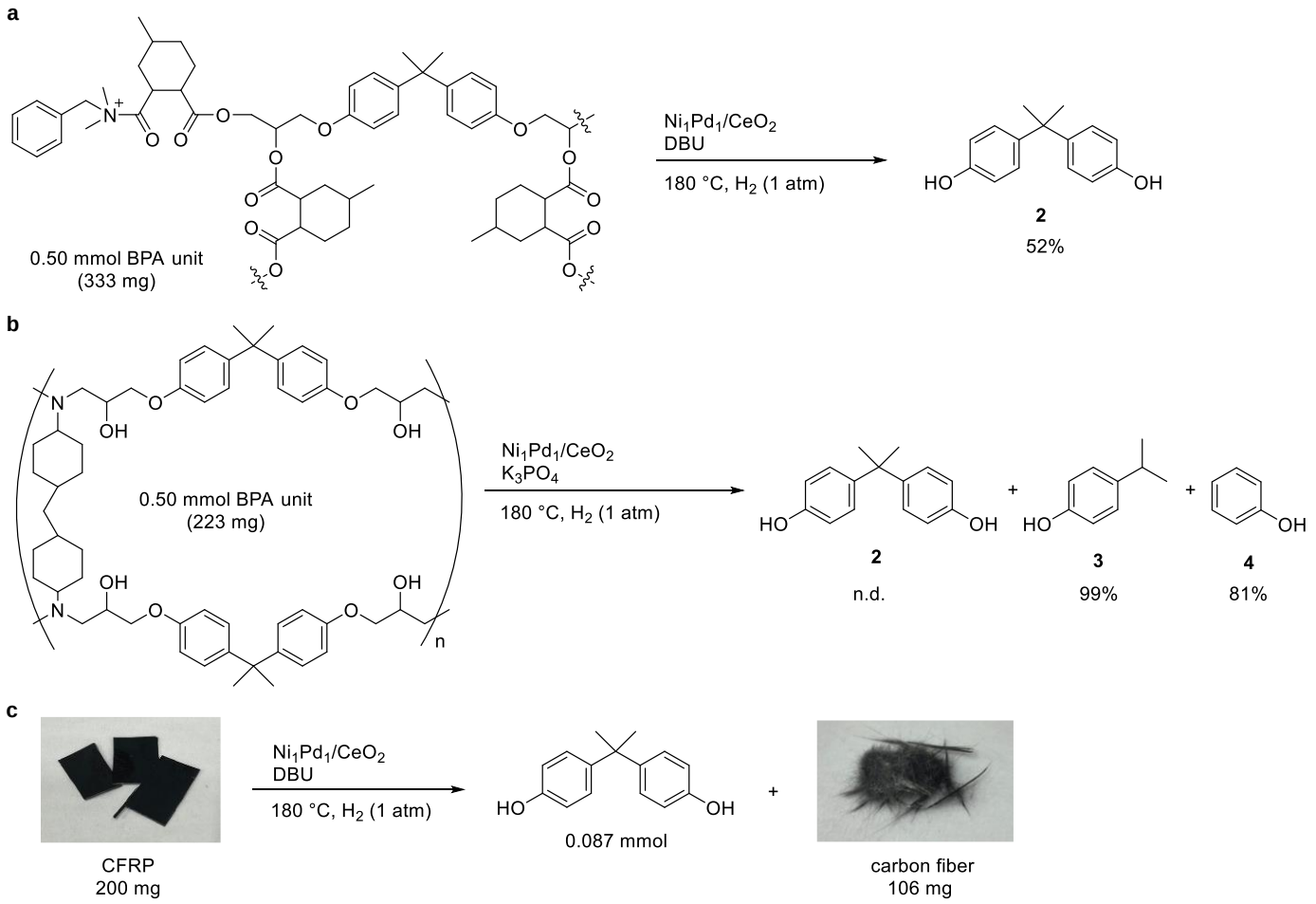

Scheme 2. Ni_1Pd_1/CeO_2-promoted hydrogenolysis of epoxy resins and decomposition of CFRP. (a) Hydrogenolysis of an acid anhydride-cured epoxy resin. Reaction conditions: resin (333 mg, 0.50 mmol BPA unit), Ni_1Pd_1/CeO_2 (100 mg), DBU (0.125 mmol), NMP (1.0 mL), 180 °C, H_2 (1 atm, balloon), 7 d. (b) Hydrogenolysis of an amine-cured epoxy resin. Reaction conditions: resin (223 mg, 0.50 mmol BPA unit), Ni_1Pd_1/CeO_2 (100 mg), K_3PO_4 (0.125 mmol), NMP (1.0 mL), 180 °C, H_2 (1 atm, balloon), 3 d. (c) Decomposition of CFRP. Reaction conditions: CFRP (200 mg), Ni_1Pd_1/CeO_2 (100 mg), DBU (0.30 mmol), NMP (2.0 mL), 180 °C, H_2 (1 atm, balloon), 3 d. The catalyst was pre-treated with 1 atm of H_2 at 300 °C for 1.0 h. Yields of the products were determined by GC analysis.

Verification of heterogeneous nature and Reuse experiment of Ni_1Pd_1/CeO_2. The heterogeneous nature of the present catalyst system was investigated as follows. For the hydrogenolysis of **5** under the conditions shown in Figure 3, the reaction completely stopped when the catalyst was removed by hot filtration at the conversion of approximately 60% (Figure 3a). In addition, when the filtrate obtained after the hydrogenolysis was analyzed by inductively coupled plasma optical emission spectroscopy (ICP-OES), Ni and Pd species were hardly detected (below the detection limit). Therefore, the Ni_1Pd_1/CeO_2 catalyst worked as a heterogeneous catalyst and the reaction proceeded on the catalyst surface.[18]

Then, the reusability of Ni_1Pd_1/CeO_2 was examined for the hydrogenolysis of **5**. The catalyst can be easily retrieved from the reaction mixture by simple filtration with >95% recovery after the hydrogenolysis. The recovered catalyst was washed with acetone, water, and ethanol followed by drying at room temperature and reducing with 1 atm of H_2 at 300 °C for 1 h before each reuse experiment. As shown in Figure 3b, the catalyst can be reused at least five times without significant loss of its performance. The HAADF-STEM analysis of Ni_1Pd_1/CeO_2 recovered after the 5th reuse experiment revealed that the Ni−Pd alloy nanoparticles remain

highly dispersed without significant aggregation of particles (Figure S4). Furthermore, by comparing the powder XRD patterns of the fresh Ni_1Pd_1/CeO_2 and that recovered after the 5th reuse experiment, the structure of the CeO_2 support remained unchanged (Figure S5). These results support the robustness of Ni_1Pd_1/CeO_2 for the hydrogenolysis.

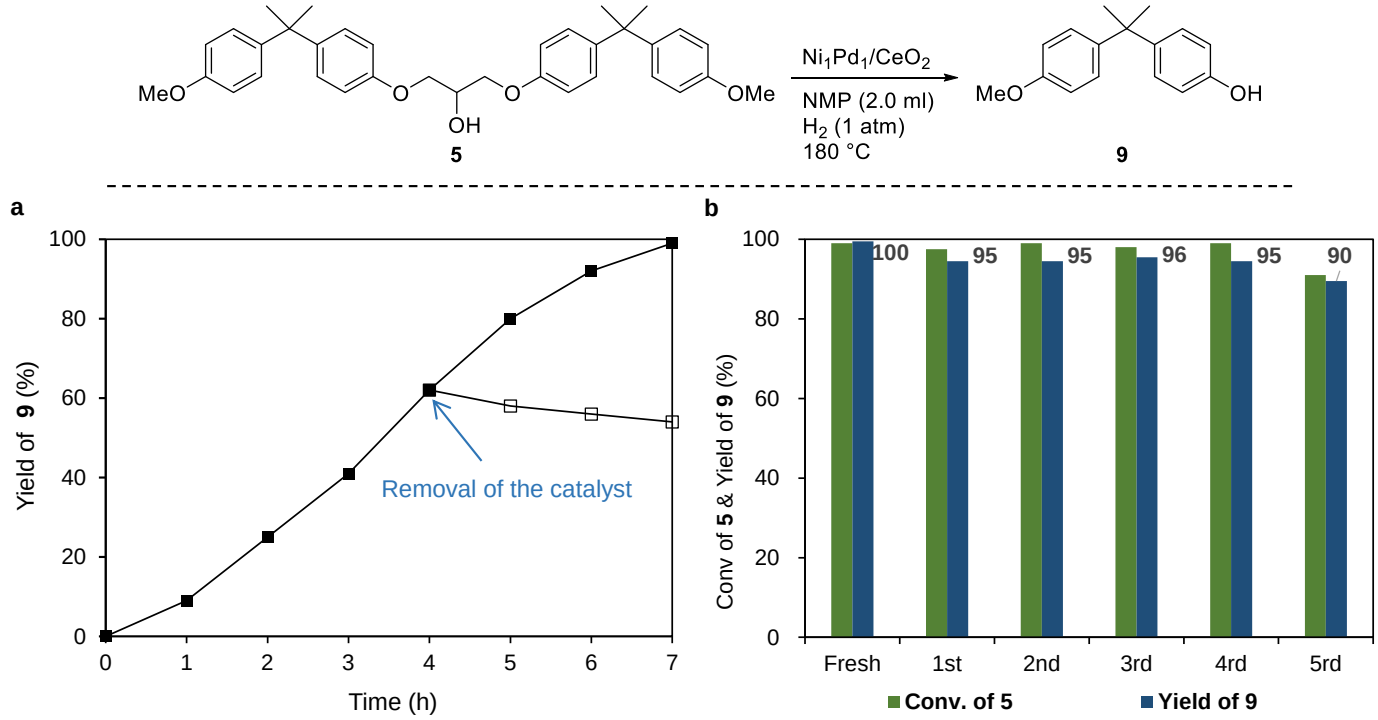

Figure 3. Leaching test and reuse of Ni_1Pd_1/CeO_2. (a) Effects of removal of the catalyst for the hydrogenolysis of **5**. The filled squares indicate the yield of **9** without removal of the catalyst, and the open squares after removal of the catalyst by hot filtration. (b) Reuse experiments. After the reaction, the catalyst was retrieved by filtration, washed with acetone, water, and ethanol, dried at room temperature, then applied to each reuse experiment. Reaction conditions: **5** (0.25 mmol), Ni_1Pd_1/CeO_2 (100 mg), NMP (2.0 mL), 180 °C, H_2 (1 atm, balloon), 7 h. The catalyst was pre-treated with 1 atm of H_2 at 300 °C for 1.0 h. The conversion and yields were determined by ^{1}H NMR and GC analysis, respectively.

Furthermore, Ni_1Pd_1/CeO_2 can be reused for the decomposition of CFRP for several times. After the decomposition experiment of CFRP, the catalyst can be easily separated from the carbon fiber by washing with acetone and water benefiting from the different shape of the catalyst and the fiber (powder *vs* fiber). The recovered catalyst was washed with acetone, water and ethanol several times followed by calcination at 300 °C under air and H_2 for 3 h and 1 h, respectively. Following these regeneration procedures, the catalyst was again subjected to the decomposition of CFRP. As shown in Table 2, the catalyst can be reused at least 5 times without notable loss of its performance. After the 5th reuse experiment, 96% of BPA was still obtained compared to the decomposition experiment using the fresh catalyst. These experiments demonstrate the potential applicability of our catalyst system for the recovery of carbon fiber and phenolic compounds from CFRP.

Table 2. Reuse of Ni_1Pd_1/CeO_2 for the decomposition of CFRP

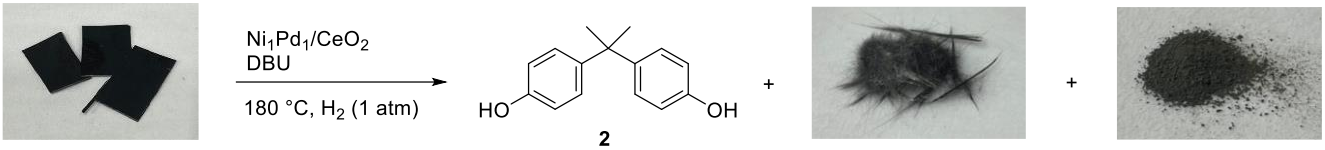

CFRP | **2** BPA | carbon fiber | recovered catalyst

Entry[a]	Catalyst	CFRP (mg)	Catalyst recovery (%)	Recovered carbon fiber (mg)	Yield of **2** (mmol)	Reusability compared to the fresh catalyst (%)
1	Fresh	200	92	106	0.087	-
2	1st reuse	192	92	106	0.080	95
3	2nd reuse	199	94	107	0.083	95
4	3rd reuse	201	96	106	0.084	97
5	4th reuse	205	92	102	0.083	93
6	5th reuse	204	93	103	0.085	96

[a]Reaction conditions: CFRP (approximately 200 mg), Ni_1Pd_1/CeO_2 (100 mg), DBU (0.30 mmol), NMP (2.0 mL), 180 °C, H_2 (1 atm, balloon), 3 d. The recovered catalyst was washed with acetone, water, and ethanol, and calcined at 300 °C under air and H_2 for 3 h and 1 h, respectively. Yield of **2** was determined by GC analysis.

Conclusion

In summary, we have successfully developed the heterogeneous Ni−Pd/CeO_2 catalyst for the hydrogenolysis of epoxy resins to recover phenolic compounds and fillers from the epoxy composites. Notably, the catalyst can be applied to the decomposition of CFRP, a widely utilized thermoset plastic used in the field such as aircrafts and automobiles. The catalyst can be recycled and reused for several times even for the decomposition of the epoxy composite. Mechanistic studies suggested that the reaction proceeds through the dehydrogenation/hydrogenolysis sequences. In addition, while the Pd-induced reduction of Ni^{2+} to Ni^0 is the key for promoting dehydrogenation of the alcohol moiety, Pd species are mainly responsible for the C−O bond hydrogenolysis. The robustness and reusability of Ni−Pd/CeO_2 for the decomposition of CFRP imply its potential application in recycling of epoxy composites.

References

1 (a) Martín, A. J., Mondelli, C., Jaydev, S. D. & Pérez-Ramírez, J. Catalytic processing of plastic waste on the rise. *Chem* **7**, 1487-1533 (2021). (b) Ellis, L. D. *et al.* Chemical and biological catalysis for plastics recycling and upcycling. *Nature Catalysis* **4**, 539-556 (2021). (c) Korley, L. T. J., Epps, T. H., Helms, B. A. & Ryan, A. J. Toward polymer upcycling-adding value and tackling circularity. *Science* **373**, 66-69 (2021). (d) Chen, X., Wang, Y. & Zhang, L. Recent Progress in the Chemical Upcycling of Plastic Wastes. *ChemSusChem* **14**, 4137-4151 (2021). (e) Lee, K., Jing, Y., Wang, Y. & Yan, N. A unified view on catalytic conversion of biomass and waste plastics. *Nature Reviews Chemistry* **6**, 635-652 (2022).

2 (a) Pham, H. Q. & Marks, M. J. Epoxy resins, in *Ullmann's Encyclopedia of Industrial Chemistry* (2005). (b) Shundo, A., Yamamoto, S. & Tanaka, K. Network Formation and Physical Properties of Epoxy Resins for Future Practical Applications. *JACS Au* **2**, 1522-1542 (2022). (c) Auvergne, R.,

Caillol, S., David, G., Boutevin, B. & Pascault, J.-P. Biobased Thermosetting Epoxy: Present and Future. *Chem. Rev.* **114**, 1082-1115 (2014). (d) Dong, M. *et al.* Multifunctional epoxy nanocomposites reinforced by two-dimensional materials: A review. *Carbon* **185**, 57-81 (2021).

3 (a) Liu, T. *et al.* Mild chemical recycling of aerospace fiber/epoxy composite wastes and utilization of the decomposed resin. *Polym. Degrad. Stab.* **139**, 20-27 (2017). (b) Liu, Y. *et al.* Closed-loop chemical recycling of thermosetting polymers and their applications: a review. *Green Chemistry* **24**, 5691-5708 (2022). (c) Jiang, Y. *et al.* Bio-based hyperbranched epoxy resins: synthesis and recycling. *Chem. Soc. Rev.* **53**, 624-655 (2024). (d Klose, L. *et al.* Towards Sustainable Recycling of Epoxy-Based Polymers: Approaches and Challenges of Epoxy Biodegradation. *Polymers* **15**, 2653 (2023). (e) Branfoot, C., Folkvord, H., Keith, M. & Leeke, G. A. Recovery of chemical recyclates from fibre-reinforced composites: A review of progress. *Polym. Degrad. Stab.* **215**, 110447 (2023). (f) Shen, Y., Apraku, S. E. & Zhu, Y. Recycling and recovery of fiber-reinforced polymer composites for end-of-life wind turbine blade management. *Green Chemistry* **25**, 9644-9658 (2023). (g) Li, Y. *et al.* Recycling of Epoxy Resins with Degradable Structures or Dynamic Cross-Linking Networks: A Review. *Ind. Eng. Chem. Res.* **63**, 5005-5027 (2024). (h) Zhang, W., Yu, H., Yin, B., Akbar, A. & Liew, K. M. Sustainable transformation of end-of-life wind turbine blades: Advancing clean energy solutions in civil engineering through recycling and upcycling. *Journal of Cleaner Production* **426**, 139184 (2023). (i) Qin, B., Liu, S. & Xu, J.-F. Reversible Amidation Chemistry Enables Closed-Loop Chemical Recycling of Carbon Fiber Reinforced Polymer Composites to Monomers and Fibers. *Angew. Chem. Int. Ed.* **62**, e202311856 (2023). (j) Zhao, Q. *et al.* Simple and Mild Method for the Recycling of Carbon-Fiber-Reinforced Bismaleimide Resin Composite Waste. *ACS Sustainable Chemistry & Engineering* **11**, 2830-2839 (2023).

4 Yang, W., Kim, K.-H. & Lee, J. Upcycling of decommissioned wind turbine blades through pyrolysis. *Journal of Cleaner Production* **376**, 134292 (2022).

5 (a) Li, J. *et al.* A promising strategy for chemical recycling of carbon fiber/thermoset composites: self-accelerating decomposition in a mild oxidative system. *Green Chemistry* **14**, 3260-3263 (2012). (b) Navarro, C. A. *et al.* Catalytic, aerobic depolymerization of epoxy thermoset composites. *Green Chemistry* **23**, 6356-6360 (2021). (c) Long, Y. *et al.* A mild and efficient oxidative degradation system of epoxy thermosets: full recovery and degradation mechanism. *Green Chemistry* **24**, 7082-7091 (2022). https://doi.org:10.1039/D2GC01678H

6 Branfoot, C., Folkvord, H., Keith, M. & Leeke, G. A. Recovery of chemical recyclates from fibre-reinforced composites: A review of progress. *Polym. Degrad. Stab.* **215**, 110447 (2023).

7 DiPucchio, R. C., Stevenson, K. R., Lahive, C. W., Michener, W. E. & Beckham, G. T. Base-Mediated Depolymerization of Amine-Cured Epoxy Resins. *ACS Sustainable Chemistry & Engineering* **11**, 16946-16954 (2023). https://doi.org:10.1021/acssuschemeng.3c04181

8 Sun, H. *et al.* Solvent–base mismatch enables the deconstruction of epoxy polymers and bisphenol A recovery. *Green Chemistry* **26**, 815-824 (2024). https://doi.org:10.1039/D3GC03707J

9 Ahrens, A. *et al.* Catalytic disconnection of C–O bonds in epoxy resins and composites. *Nature* **617**, 730-737 (2023).

10 Liao, Y., Takahashi, K. & Nozaki, K. Nickel-Catalyzed C(sp3)–O Hydrogenolysis via a Remote-Concerted Oxidative Addition and Its Application to Degradation of a Bisphenol A-Based Epoxy Resin. *J. Am. Chem. Soc.* **146**, 2419-2425 (2024).

11 (a) Eid, N., Ameduri, B. & Boutevin, B. Synthesis and Properties of Furan Derivatives for Epoxy

Resins. *ACS Sustainable Chemistry & Engineering* **9**, 8018-8031 (2021). (b) Türel, T., Dağlar, Ö., Eisenreich, F. & Tomović, Ž. Epoxy Thermosets Designed for Chemical Recycling. *Chemistry – An Asian Journal* **18**, e202300373 (2023).

12 (a) Alonso, D. M., Wettstein, S. G. & Dumesic, J. A. Bimetallic catalysts for upgrading of biomass to fuels and chemicals. *Chem. Soc. Rev.* **41**, 8075-8098 (2012). (b) Cheng, C., Shen, D., Gu, S. & Luo, K. H. State-of-the-art catalytic hydrogenolysis of lignin for the production of aromatic chemicals. *Catalysis Science & Technology* **8**, 6275-6296 (2018). (c) Shivhare, A. *et al.* Hydrogenolysis of Lignin-Derived Aromatic Ethers over Heterogeneous Catalysts. *ACS Sustain. Chem. Eng.* **9**, 3379-3407 (2021). (d) Yun, Y. S., Berdugo-Díaz, C. E. & Flaherty, D. W. Advances in Understanding the Selective Hydrogenolysis of Biomass Derivatives. *ACS Catalysis*, 11193-11232 (2021). (e) Liu, L. & Corma, A. Bimetallic Sites for Catalysis: From Binuclear Metal Sites to Bimetallic Nanoclusters and Nanoparticles. *Chem. Rev.* **123**, 4855-4933 (2023).

13 (a) Zakzeski, J., Bruijnincx, P. C. A., Jongerius, A. L. & Weckhuysen, B. M. The Catalytic Valorization of Lignin for the Production of Renewable Chemicals. *Chem. Rev.* **110**, 3552-3599 (2010). (b) Ragauskas, A. J. *et al.* Lignin Valorization: Improving Lignin Processing in the Biorefinery. *Science* **344**, 1246843 (2014). (c) Barta, K. & Ford, P. C. Catalytic Conversion of Nonfood Woody Biomass Solids to Organic Liquids. *Acc. Chem. Res.* **47**, 1503-1512 (2014). (d) Zaheer, M. & Kempe, R. Catalytic Hydrogenolysis of Aryl Ethers: A Key Step in Lignin Valorization to Valuable Chemicals. *ACS Catal.* **5**, 1675-1684 (2015). (e) Zhang, B., Meng, Q., Liu, H. & Han, B. Catalytic Conversion of Lignin into Valuable Chemicals: Full Utilization of Aromatic Nuclei and Side Chains. *Acc. Chem. Res.* **56**, 3558-3571 (2023). (f) De Smet, G., Bai, X. & Maes, B. U. W. Selective C(aryl)–O bond cleavage in biorenewable phenolics. *Chem. Soc. Rev.* (2024).

14 (a) Sergeev, A. G., Webb, J. D. & Hartwig, J. F. A heterogeneous nickel catalyst for the hydrogenolysis of aryl ethers without arene hydrogenation. *J. Am. Chem. Soc.* **134**, 20226-20229 (2012). (b) He, J., Zhao, C. & Lercher, J. A. Ni-catalyzed cleavage of aryl ethers in the aqueous phase. *J. Am. Chem. Soc.* **134**, 20768-20775 (2012). (c) Molinari, V., Giordano, C., Antonietti, M. & Esposito, D. Titanium nitride-nickel nanocomposite as heterogeneous catalyst for the hydrogenolysis of aryl ethers. *J. Am. Chem. Soc.* **136**, 1758-1761 (2014). (d) Sturgeon, M. R. *et al.* Lignin depolymerisation by nickel supported layered-double hydroxide catalysts. *Green Chemistry* **16**, 824-835 (2014). (e) Stavila, V. *et al.* MOF-Based Catalysts for Selective Hydrogenolysis of Carbon–Oxygen Ether Bonds. *ACS Catal.* **6**, 55-59 (2015). (f) Gao, F., Webb, J. D. & Hartwig, J. F. Chemo- and Regioselective Hydrogenolysis of Diaryl Ether C–O Bonds by a Robust Heterogeneous Ni/C Catalyst: Applications to the Cleavage of Complex Lignin-Related Fragments. *Angew. Chem. Int. Ed.* **55**, 1474-1478 (2016). (g) Schwob, T. *et al.* General and selective deoxygenation by hydrogen using a reusable earth-abundant metal catalyst. *Sci. Adv.* 5, eaav3680 (2019). (h) Qi, L. *et al.* Unraveling the Dynamic Network in the Reactions of an Alkyl Aryl Ether Catalyzed by Ni/γ-Al_2O_3 in 2-Propanol. *J. Am. Chem. Soc.* **141**, 17370-17381 (2019). (i) Wang, M. *et al.* The Critical Role of Reductive Steps in the Nickel-Catalyzed Hydrogenolysis and Hydrolysis of Aryl Ether C−O Bonds. *Angew. Chem. Int. Ed.* **59**, 1445-1449 (2020). (j) Jiang, L., Xu, G., Fu, Y. Catalytic Cleavage of the C–O Bond in Lignin and Lignin-Derived Aryl Ethers over Ni/AlP_yO_x Catalysts. *ACS Catal.* **12**, 9473-9485 (2022).

15 Bligaard, T. *et al.* The Brønsted–Evans–Polanyi relation and the volcano curve in heterogeneous catalysis. *J. Catal.* **224**, 206-217 (2004).

16 (a) Zhang, J. *et al.* A Series of NiM (M = Ru, Rh, and Pd) Bimetallic Catalysts for Effective Lignin

Hydrogenolysis in Water. *ACS Catalysis* **4**, 1574-1583 (2014). (b) Zhang, J. *et al.* Highly efficient, NiAu-catalyzed hydrogenolysis of lignin into phenolic chemicals. *Green Chemistry* **16**, 2432-2437 (2014). (c) Kim, J. K., Lee, J. K., Kang, K. H., Song, J. C. & Song, I. K. Selective cleavage of CO bond in benzyl phenyl ether to aromatics over Pd–Fe bimetallic catalyst supported on ordered mesoporous carbon. *Applied Catalysis A: General* **498**, 142-149 (2015). (d) Zhang, J.-w., Cai, Y., Lu, G.-p. & Cai, C. Facile and selective hydrogenolysis of β-O-4 linkages in lignin catalyzed by Pd–Ni bimetallic nanoparticles supported on ZrO2. *Green Chemistry* **18**, 6229-6235 (2016). (e) Zhang, J. *et al.* Rh nanoparticles with NiOx surface decoration for selective hydrogenolysis of CO bond over arene hydrogenation. *J. Mol. Catal. A: Chem.* **422**, 188-197 (2016). (f) Zhang, J.-w., Lu, G.-p. & Cai, C. Self-hydrogen transfer hydrogenolysis of β-O-4 linkages in lignin catalyzed by MIL-100(Fe) supported Pd–Ni BMNPs. *Green Chemistry* **19**, 4538-4543 (2017). (g) Bulut, S. *et al.* Efficient cleavage of aryl ether C–O linkages by Rh–Ni and Ru–Ni nanoscale catalysts operating in water. *Chemical Science* **9**, 5530-5535 (2018). (h) Zhu, C. *et al.* Bimetallic effects in the catalytic hydrogenolysis of lignin and its model compounds on Nickel-Ruthenium catalysts. *Fuel Process. Technol.* **194**, 106126 (2019).

17 Kuang, X., Zhou, Y., Shi, Q., Wang, T. & Qi, H. J. Recycling of Epoxy Thermoset and Composites via Good Solvent Assisted and Small Molecules Participated Exchange Reactions. *ACS Sustainable Chemistry & Engineering* **6**, 9189-9197 (2018).

18 Sheldon, R. A., Wallau, M., Arends, I. W. C. E. & Schuchardt, U. Heterogeneous Catalysts for Liquid-Phase Oxidations: Philosophers' Stones or Trojan Horses? *Acc. Chem. Res.* **31**, 485-493 (1998).

Acknowledgements

This work was supported by JST ERATO JPMJER2103, and JSPS KAKENHI JP24K01253, JP23H04905. A part of this work was conducted at the Advanced Characterization Nanotechnology Platform of the University of Tokyo, supported by “Nanotechnology Platform” of the Ministry of Education, Culture, Sports, Science and Technology (MEXT), Japan. The XAFS experiments at SPring–8 were carried out with the approval (proposal no. 2023A2023) of the Japan Synchrotron Radiation Research Institute (JASRI). We are grateful to S.Iwahana (Toray Industries, Inc.) and A.Masunaga (Toray Industries, Inc.) for kindly providing the CFRP sample.

Author contributions

X.J. and K.Nozaki. designed the studies and conceived the main idea. Y.H. and Y.Y. executed all the experimental works except for the XAFS measurements. K.Nomoto, H.M., and T.S. measured and analyzed the XAS spectra. All authors discussed the results and wrote the paper.